

Calculating the Force Exerted by Simple Molecular Machines

Evangelos Bakalis^{1,2} and Francesco Zerbetto^{1,2}

1) *Dipartimento di Chimica "G. Ciamician," Università di Bologna, Via F. Selmi 2, I-40126
Bologna, Italy*

2) *Consorzio Interuniversitario Nazionale per la Scienza e Tecnologia dei Materiali – Sezione
di Bologna*

E-mail: ebakalis@gmail.com, francesco.zerbetto@unibo.it

Phone: 0039 051 2099473, Fax: +39 051 2099456

(Received February 10, 2011)

Abstract

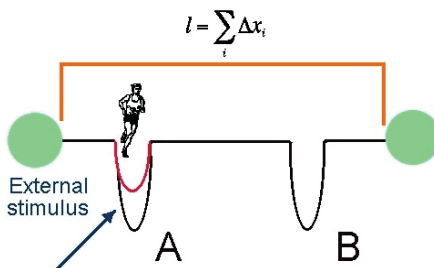
Many biological and artificial molecular machines start their operation with an external stimulus/input that moves them out of equilibrium and places them into a “prepared state”. Their functioning sets off by exploiting random fluctuations of their environment. The initial random motion is then organized to achieve net directional displacement. While the chemical mechanisms behind the motion are often clear, predicting and extracting properties connected to their dynamical evolution is difficult. The determination of the force and the efficiency of the system is a crucial step towards their systematic design and exploitation. By using a discrete Markovian stochastic model whose parameters are matched to chemical quantities such as interatomic distances and energy differences, we describe the dynamics of the simplest molecular machine system, a double-well system where the “prepared state” is slightly higher in energy than the final equilibrium state and evolves towards this thermodynamically stable state. We determine the form of the time-dependent force exerted on the environment, the efficiency of the machine, while some general rules for the design of nanomachines are obtained and discussed. The model captures the basic features of the machine’s operation, while it can be extended to describe systems consisting of more than two states.

1. Introduction

The kernel of a machine is its motor that is something causing motion that ultimately generates useful work via the variation in time of either the position or the orientation of one of its components. As in the case of macroscopic machines, also molecular machines are made by components, one of which is set in motion with respect to the others by an external stimulus that moves the system out of equilibrium. This mechanical motion is the main or perhaps the only similarity between nanomachines and macroscopic machines. Indeed nanomachines are not simply down-scaled versions of their macroscopic counterparts and their functioning is based on an entirely different basis. For molecular machines in the over-damped limit, rectification of Brownian motion is the *modus operandi*, at odds with macroscopic machines where the same continuous rectification, at equilibrium, would ultimately imply violation of second law of thermodynamics.

It is accepted that the design of Brownian motors necessitates spatio-temporal asymmetry, and out-of-equilibrium conditions. The second law of thermodynamics requires that structural features alone -no matter how cleverly designed- cannot bias the Brownian motion present at equilibrium [1-2]. A gradient either thermal or of chemical nature can cause directional motion and generate useful work. In chemistry and biology, the realization of nano-scale thermal gradients to drive significant motion is often not realistic. However, Brownian motion can be biased even in isothermal systems, if energy is supplied by external fluctuations [3-5] or by chemical reactions [6-7]. The direction of motion is governed by the combination of the local spatial anisotropy of the potential energy, the diffusion coefficient of the particle in the medium, and the specific details of how the external stimulus is introduced [8].

Simple molecular machines that operate at the nanometer-scale are becoming a reality [9-11]. In the simplest formulation, they can be represented by two potential energy minima where the molecule/motor has different configurations/structures. In the initial situation of equilibrium, only the deepest minimum, located at x_0 , is populated, $P(x,0)=\delta(x-x_0)$, where P is the probability density distribution function at the initial point in time, $t=0$, and $\delta(x-x_0)$ is the Dirac Delta function.



Scheme 1. Two-minima molecular machines schematic representation. The initially more stable minimum, A, is activated by an external stimulus and the machine represented by a walker moves by executing Brownian motion towards the second minimum, B, as it tries to reach equilibrium; l is the length of the pathway used by the motor and Δx is the stride of the walker or space step. The pathway of the motor is restricted between the two sidewalls close to A and B.

An external stimulus, be it light absorption, pH variations, or electrons transfer modifies the chemical nature of the configuration and increases the energy of minimum above that of the secondary minimum [12], B, see scheme 1. The newly established energy difference between the structures of the two minima is then available for transduction if the barrier between the two minima is thermally accessible. The molecular re-arrangement that brings the system to equilibrium is one-directional and exerts a net force on the environment. An important issue towards the exploitation of an artificial molecular machine is the amount of force that it can exert -after it is started and off-equilibrium conditions are set. The force exerted by a nanomachine on its environment can be recorded by an AFM experiment where the force is measured via the AFM tip. Most of the theoretical work relates to forces exerted against an external load since there is a direct link between theoretical predictions and experimental evidence. In that case, part of the available work is converted into some useful form. Even very recently, some of the best estimates of the exerted force, an upper bound limit, were carried out under the assumption that all of the free energy could be converted into mechanical work moving the motor through distance d . The approach considers neither the influence of the environment, nor dissipation or entropic effects. In practice, the exerted force was calculated as, $F_{\max} = \Delta G_0 / d$, the ratio of the free energy gained by the particle during the motion, ΔG_0 , divided the length of the path, d , [13]. For a diffusing particle subject to an external load and at thermal equilibrium, the Einstein force is the most elegant expression. It connects temperature, diffusion coefficient, drift velocity, and is equal to $F_E = k_B T v / D$, where

$k_B T$ is Boltzmann's constant times the temperature of the bath, and v is the mean velocity of the walker that represents the engine when it has reached the steady state characterized by constant flux [14].

On the other hand, there are systems where a systematic external load does not exist, but is only present at specific sites of the environment. In these cases the particle transits from random into either partially or fully ordered motion [8] and all the useful work is dissipated and cannot be used for other purposes. The evolution in time of such systems can be recorded by using time-resolved vibrational spectroscopy techniques [15], which makes it possible to decipher how systems that evolve in the nanosecond scale work. Recently, the operational mechanism of a two-station rotaxane-based molecular machine was recorded by using such techniques and an interesting analysis was performed [16]. The discussion reported in the present work is applicable to any bi-stable system, it can be extended to include more potential energy minima and has the intent of linking molecular kinetic and thermodynamic details to quantities, such as mean displacement, exerted force and current flux that are able to describe the functioning of a nanomachine at the molecular-level. Moreover, the suggested theoretical framework is able to explain findings that are obtained by time-resolved vibration spectroscopy experiments.

2. The picture and its details

The dynamics of many molecular rearrangements can be described as a one-dimensional random walk between two configurations. The presence of sites/vertices -not minima- characterizes the pathway. They can be located arbitrarily or have a physical meaning. For instance in a machine where the motor functions through the torsion about a chemical bond [17], they can be positioned every few degrees. Alternatively, in machines where the motor is a molecular ring that walks along an alkyl chain, a site may correspond to the location of a CH_2 group [12]. The separation between the sites, Δx , is the stride of the walker.

In the ideal random walk, there are neither barriers nor wells along the walk. The walker jumps randomly from the site it occupies, i.e., the structure of the molecule, to one of the nearest neighboring sites with transition probability $p_{ij} = 1/2$ for $j = i \pm 1$, and 0 otherwise. For simplicity, x is the space variable both in the discrete and in the continuous (see below)

model. After time $t = n\tau$, with n number of steps and τ is the time step, the probability to find the walker at a site, given the initial distribution, $P(x_0, 0) = 1$, is described by the Chapman-Kolmogorov recursive relation [18], which for a one-dimensional system reads

$$P(x, n) = \frac{1}{2} \{P(x - \Delta x, n-1) + P(x + \Delta x, n-1)\} \quad (1)$$

In the iteration of equation (1) in time represented by n , the probability depends only on that obtained at the previous time step, i.e., Markovian stochastic process, and for a large number of steps, it yields the normalized Gaussian distribution.

Equation (1) becomes more complicated when potential energy minima, or wells, are present (17)

$$P(x, n) = \frac{1}{2} \{P(x - \Delta x, n-1) + P(x + \Delta x, n-1)\} \left(1 + \sum_i k_i \delta_{x, x_i} \right) \quad (2)$$

the additional term $\sum_i k_i \delta_{x, x_i}$ in equation (2) accounts for the effects of the potential energy wells on the motion of the walker and makes the transition probability for the motion direction-dependent: it is easier to jump into the well than out of it. In the equation, δ_{x, x_i} , is Kronecker delta, which is one if site x_i is the location of the minimum, and is zero otherwise; $k_i = -1 + \exp(-u_{i,d})$ contains the potential energy, $u_{i,d}$ is a dimensionless, temperature-weighted quantity (subscript d stands here for “discrete”). In practice, the site-to-site transition probabilities required for application of equation (2) are $\frac{1}{2D}$, with D is the dimensionality of the space, if the site reachable by the walker is “free”, and $\frac{1}{2D} \exp(-u_{i,d})$ if it is “home” to the potential energy well.

In equation (2), $P(x, n)$ still depends only on the probability distribution obtained at the previous time step, but is no longer normalized and care must be exerted after each step to normalize it. Iteration of equation (2) is used to determine the probability distribution at each step in time. An example of the application of equation (2) is given in supporting information material.

The iteration in time of equation (2) requires three types of quantities: the time step τ , the space step Δx , and $u_{i,d}$. The space step Δx is related to the structure of the molecular

machine and is defined accordingly. The relation $\tau = \Delta x^2 / 2D$ is used to define τ , where D is the diffusion coefficient. The critical quantity is $u_{i,d}$ which is often used as an empirical parameter. Its effect on the dynamics is usually investigated without attempting a direct correlation with real-life molecules. In order to make the match, we notice that equation (2) has a continuum counterpart in a generalized diffusion type equation [19-22]

$$\frac{\partial}{\partial t} P(x, t) = D \frac{\partial^2}{\partial x^2} P(x, t) - UP(x, t) \quad (3)$$

where D is the diffusion coefficient, U expresses the rate of visits (in units of inverse time), and accounts for the extra interactions that the presence of barriers or potential energy minima bring on the random motion. It can take positive/negative values reflecting the decrease/increase of the number of visits of the motor to the area of the local inhomogeneity (barrier or potential energy well). This frequency is always determined in comparison with the frequency of visits of the motor to a prescribed area in the absence of barrier/potential energy well where the interaction potential is nil and equation (3) returns to the classical diffusion equation. U is parametric in space and reads

$$U = \bar{u}_c \sum_{i=1}^m \delta(x - x_i)$$

$$\bar{u}_c = u_c / t_{eq}$$

$$u_c = \int_0^{\infty} dx \left(1 - \text{Exp}[-V(x) / k_B T] \right) \quad (4)$$

where, x_i denotes the position of the potential energy minima, the index c stands for continuum, t_{eq} is the time that the system takes to reach equilibrium (see supporting information material about the parameter \bar{u}_c), the integral can be calculated either analytically or numerically once the potential energy curve, $V(x)$, and the temperature have been defined. $V(x)$ is here described by a delta function potential and this choice is physically reasonable if the minima exist because of short range interactions [22-27], such as hydrogen bonds, that are usually severed by a displacement of a fraction of an Ångstrom in scheme 1 [28-30].

Equation (3), as well its discrete counterpart, has been successfully applied to describe a plethora of kinetic problems [31-39]. It must be noticed that eq(2) and eq(3) are not the

same. In equation (2) the quantity $P(x, n)$ expresses probability, while in eq.(3) the quantity $P(x, t)$ expresses probability density function. Although both describe qualitatively well the same phenomena there is no quantitative agreement of the results obtained with them [40]. Equations (2) and (3) coincides if we make the following matches

$$D = \lim_{\Delta x, \tau \rightarrow 0} \frac{\Delta x^2}{2\tau} \quad (5)$$

and (41)

$$u_d = \lim_{\Delta x, \tau \rightarrow 0} (-\ln(1 - (\tau / \Delta x) \bar{u}_c)) \quad (6)$$

where τ is the time step needed by the walker to perform a space step, while u_d is dimensionless. If conditions (5) and (6) are not fulfilled, one can still match the dynamics of the two equations by setting $u_d = -\ln(1 - b(\tau / \Delta x) \bar{u}_c)$ and $\tau = \frac{\Delta x^2}{2D}$ and by varying the empirical factor b .

In practice, in order to use equation (2) to investigate the dynamics, we applied equations (2) and (3) to a system with a single minimum and varied b until the mean displacement of two dynamics coincided.

In the continuous model and for single potential energy minima the mean displacement is given by [19]

$$\langle (x - x_0) \rangle(t) = |x_1 - x_0| \frac{g(\bar{u}_c, D, x_1, x_0, t)}{1 + g(\bar{u}_c, D, x_1, x_0, t)} \quad (7)$$

where x_0 is the initial position of the walker, x_1 is position of the energy minimum, D is the diffusion coefficient, and

$$g(\bar{u}_c, D, x_1, x_0, t) = \exp\{(\bar{U}_c + X_p)^2 - X_p^2\} \cdot \operatorname{erfc}\{\bar{U}_c + X_p\} - \operatorname{erfc}\{X_p\},$$

with $\bar{U}_c = \bar{u}_c \sqrt{t / 4D}$, and $X_p = |x_1 - x_0| / \sqrt{4Dt}$

In the discrete model, the mean displacement is given by

$$\langle x(n\tau) - x_0 \rangle = \sum_{k=-n}^n (x(k) - x_0) P(x(k), n\tau) \quad (8)$$

where n is the number of steps of time length τ , k runs over the sites, and $x(k) = x_0 + k\Delta x$. Since the continuum model implies infinitesimally small space steps, we use the smallest possible chemical space step that corresponds to $\Delta x = 1\text{\AA}$.

Figure 1 compares the results of the two models at $T=298\text{ K}$, for a diffusing particle that starts its motion 6 \AA away from a potential energy minimum of 14 kcal mol^{-1} in a medium with viscosity coefficient $\eta=10^{-3}\text{ Pa sec}$. The two dynamics coincide when the empirical parameter b is set to 1.164.

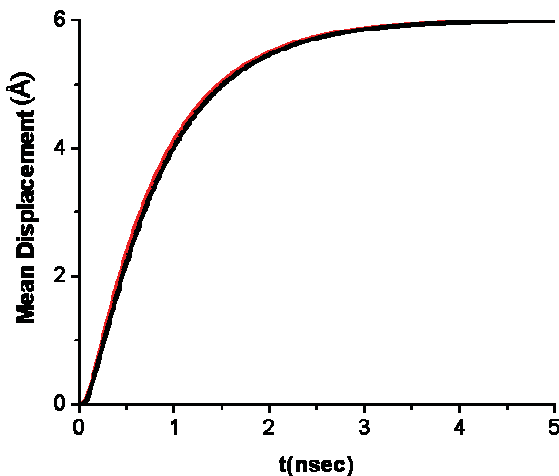


Figure 1. Mean displacement at room temperature for the continuous (black line) and discrete (red line) representations for a diffusing particle that starts its motion 6 \AA away from a potential energy minimum of 14 kcal mol^{-1} . The system is embedded in a typical organic solvent with viscosity coefficient $\eta=10^{-3}\text{ Pa sec}$. The two dynamics coincide if $b=1.164$.

At 298, 310, and 320 K, the optimal b parameter was 1.164, 1.043 and 1.020. We then used the values of u_d , eq.6, in the simulation of the off-equilibrium dynamics. A set of \bar{u}_c and u_d values for different temperatures and depth of the potential was calculated, see ‘table 1’ for more details together with ‘table 2’ for time steps.

Table 1. \bar{u}_c , m s⁻¹, and u_d , dimensionless, values for different temperatures, K, and binding energies of the wells, kcal mol⁻¹, calculated for t_{eq} = 1 sec.

	Binding energy	-14	-13	-12	-11	-10	-9	-8	-7
T									
\bar{u}_c									
298		-1.844	-0.3408	-0.0630	-0.0116	-2.15 10 ⁻³	-3.98 10 ⁻⁴	7.35 10 ⁻⁵	-1.36 10 ⁻⁵
310		-0.7385	-0.1457	-0.02875	-0.0057	-1.12 10 ⁻³	-2.20 10 ⁻⁴	-4.35 10 ⁻⁵	-8.6 10 ⁻⁶
320		-0.3631	-0.0754	-0.0156	-0.00325	-6.74 10 ⁻⁴	-1.40 10 ⁻⁴	-2.9 10 ⁻⁵	-6.02 10 ⁻⁶
u_d									
298		-0.152	-0.03	-5.6 10 ⁻³	-1 10 ⁻³	-1.91 10 ⁻⁴	-3.5 10 ⁻⁵	-6.53 10 ⁻⁶	-1.21 10 ⁻⁶
310		-0.055	-0.011	-2.2 10 ⁻³	-4.4 10 ⁻⁴	-8.6 10 ⁻⁵	-1.7 10 ⁻⁵	-3.33 10 ⁻⁶	-6.58 10 ⁻⁷
320		-0.026	-5.4 10 ⁻³	-1.1 10 ⁻³	-2.4 10 ⁻⁴	-4.9 10 ⁻⁵	-1 10 ⁻⁵	-2.01 10 ⁻⁶	-4.36 10 ⁻⁷

Table 2. Diffusion coefficients and time steps used at the various temperatures. The model uses $\Delta x = 1, 2, 3, 6$ and $\tau = \Delta x^2 / 2D$.

	space step, Δx (\AA)	time step, τ (ps)	$D(\text{m}^2/\text{sec})10^{-10}$	b
T=298 K	1	7.64	6.55	1.164
	2	30.54	6.55	
	3	68.72	6.55	
	6	274.88	6.55	
T=310 K	1	7.34	6.81	1.043
	2	29.36	6.81	
	3	66.10	6.81	
	6	264.245	6.81	
T=320 K	1	7.11	7.03	1.020
	2	28.44	7.03	
	3	64	7.03	
	6	255.99	7.03	

3. Calculating the properties of the system

The properties of the system (molecule plus the environment) appear in (i) \bar{u}_c and u_d , which quantify the binding energy of the minima; (ii) the length of the pathway, $l = \sum_i \Delta x_i$; (iii) the diffusion coefficient, D , which is connected to mobility, μ , via the Einstein relation $D = \mu k_B T$, $\mu = 1/2\pi\eta r$, in a way that ensures thermal equilibrium since the temperature increase due to conversion of supplied energy is negligible, η is the viscosity of the medium; and (iv) the size of the walker, with radius r .

Time dependent properties for colloidal particles have been obtained before with different models [39]. Apart for the mean displacement of equation 8, which shows the directionality of the motion, two more interesting quantities are the non-equilibrium Gibbs entropy

$$S(n\tau) = -k_B \sum_{k=-n}^n P_{norm}(x(k), n\tau) \ln(P_{norm}(x(k), n\tau)) \quad (9)$$

together with the current flux in time or drift velocity [41],

$$J(n\tau) = v_{inst} \sum_i (w_{Ri} P_{norm}(x_i - \Delta x, (n-1)\tau) - v_{inst} \sum_i (w_{Li} P_{norm}(x_i + \Delta x, (n-1)\tau)) \quad (10)$$

where, v_{inst} is the instantaneous velocity of the walker which is equal to the space step divided by the time step, and has a meaning only in the discrete model, its equivalent in continuous model goes to infinity (non-differentiable trajectories). The x_i are the sites of the potential energy minima, w_{Ri} and w_{Li} are the transition probabilities to the right and to the left of site i , and $P_{norm}(x_i, x_0, n\tau)$ is the normalized probability at site i after n time steps. If one considers the mass of the walker small, ignores inertial effects, and considers large the friction coefficient, γ , $\gamma = 2\pi\eta r$, then the exerted force evaluated according to Newton's second law is equal to

$$F_{exerted}(n) = \gamma J(n) \quad (11)$$

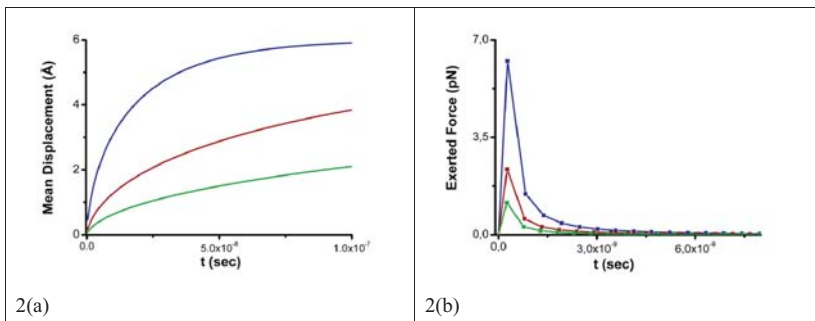
and takes the form $F_{exerted}(n) = \frac{k_B T}{D} J(n)$ that is similar to the Einstein Force, but here the $J(n)$ does not correspond to steady state, while, the power output reads [43]

$$P_{out}(t) = \gamma J^2(t) \quad (12)$$

To calculate the efficiency, f , of the system one can define $f = \frac{W_{out}}{W_{in}}$, W_{in} is the energy available from the system or energy difference between the wells, while W_{out} is the useful work done by the system, $W_{out} = \int_0^{t_{eq}} F_{exe}(t)J(t)dt$, with t_{eq} the time needed for the walker to reach equilibrium.

4. Results and discussion

In the free case, the random walker that physically represents the nanoengine starts its motion from the initial site and jumps to one of its nearest neighbor sites –not minima– with an equal transition probability. In the presence of potential energy minima, the transition probability is modified. For the practical application of the algorithm of eq.2, it is necessary to specify the energy values of the minima in scheme 1. In analogy with some artificial molecular machines,[11-13,28-30] after off-equilibrium conditions are set, the walker is positioned at a site with a potential energy of $-10 \text{ kcal mol}^{-1}$ and the second minimum has a potential energy well of $-14 \text{ kcal mol}^{-1}$. The length of the lattice, or pathway, is 6 \AA between the minima with 2 additional Ångstroms to the sides, the viscosity is 10^{-3} Pa s (for typical organic solvents); and the size of the walker is 1 nm . These values are typical of what is achieved and discussed in several papers where the prepared unbalanced state is obtained photochemically [28-30]. A further parameter that influences the functioning of the machine is the step of the walker, Δx . As already noticed elsewhere [44], Δx can have a physical meaning, which is here the passing of a chemical group by the walker.



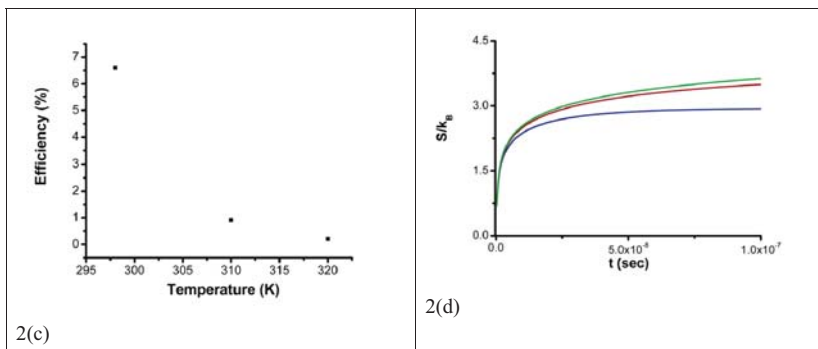


Figure 2. After setting the system off equilibrium, a random walker moves from a 10 kcal mol⁻¹ minimum to a 14 kcal mol⁻¹ minimum that is located 6 Å away. Blue lines for T=298 K, red lines for T=310 K, green lines for T=320 K. 2(a) Mean displacement of the walker, 2(b) Force exerted on the walker by its environment, 2(c) Efficiency, 2(d) Entropy production in time.

Back of the envelope calculations show that the escape from a potential energy well of -10 kcal mol⁻¹ is in the sub-microsecond regime. For a path-length of the order of a nanometer, the velocity of the walker is ~0.01 mm s⁻¹, which also happens to be one of the largest achieved with a class of nanomotors that are based on catalytic reactions [45].

The set of figures 2 present the results for a large stride of $\Delta x = 6$ Å and for three different temperatures T=298, 310 and 320 K. Smaller strides of $\Delta x = 1, 2,$ and 3 Å are discussed in the text.

Figure 2(a) shows the mean displacement of the walker, by applying equation (8), as a function of temperature, over 0.1 μs. If the second well is deep enough, at equilibrium, the final mean displacement must be the same at all temperatures and must be equal to the pathway length between the two minima. At T=298 K, after 0.1 μs, the walker is fully localized at the second minimum. As the temperature goes up the walker needs more time to become localized because it can easier escape also from the final deeper well and several visits occur before full localization. In practice, higher temperatures promote backscattering from the deeper energy well.

Figure 2(b) presents the force exerted on the walker by its environment as function of time for the same temperatures of figure 2(a). The environment exerts its force on the walker in a different way than the familiar spatial derivative of the potential energy. In the present

model, the potential sites are point-like and their spatial derivatives are meaningless. The environment exerts forces on the walker via memory effects, which are reflected on the walker's probability distribution. If the space is isomorphic, then sites that are located symmetrically with respect to the starting point have the same probability that the walker will be found on them. If potential/barrier sites are present, symmetry is broken and some sites have greater probability of a visit by the walker. It is then possible to describe the dynamics in terms of memory effects that drive the probability distribution towards a direction; memory effects may lead to anomalous diffusion or even localization [19,46]. The process is similar to deterministic forces that drive a particle towards the minimum of a potential difference. The action of a potential energy difference on a particle that executes random motion is reflected on the memory that the particle retains during its motion, and its average behavior is obtained by integrating over all the entire space where the particle can be found during motion. The force exerted by the walker against its environment is the opposite of the force exerted by the environment on it, in agreement with Newton's third law.

The exerted force on the walker and its total flux, or drift velocity, have the same structure, independently of the choice of the space step, as is expected according to equation (11). The main variations take place during the first 2 ns. For $\Delta x = 6 \text{ \AA}$, the maximum value appears at the first step as the walker jumps into the more attractive minimum. Subsequently, the force decays exponentially due to the backscattering (see above). In practice, the walker reaches the second minimum and returns back with a higher probability the higher the temperature.

By comparing the mean displacement and the exerted force on the walker, figures 2(a) and 2(b), we can obtain some information on how the walker exerts force on the system, the importance of the initial population of the prepared state, and the role of the deeper minimum. The maximum value of the exerted force on the walker is reached during the first visits to the second minimum, i.e., the deeper potential well. At the same time, the mean displacement, a quantity that shows how the initial population shifts, indicates that the distribution is very close to its initial position. The walker after its first visit to the second minimum retains a memory, reflected on its probability distribution, of the existence of the local inhomogeneity. If the potential site is attractive the movement becomes favoured by the walker, and this situation is similar to what was described by the inventive phrase "Elephants can always remember" [47]. On the other hand, the walker also has memory of its initial distribution. This second kind of memory pushes the walker backward, and as the walker tries to escape

from the second minimum, it exerts on its environment a force that is opposite to its net displacement. The force exerted by the walker on its environment is therefore the result of the competition between two different memory effects, the memory of its initial distribution that pushes back the walker, and the memory due to potential energy minimum that makes a direction preferable for the motion. The force exerted by the walker for the simplest case of a molecular machine consisting of two stations is always driven by the deepest minimum. This picture is enhanced by the results listed in ‘table 4’, where three different pairs of potential wells have been chosen, with the deepest well that is always the same. We find that the force exerted is always the same and is determined by the deepest well. The walker, before reaching the second minimum, does not exert force on its environment. The sites around the initial population, which is localized at the first minimum, are symmetric with respect to it, thus the forces exerted to the left and to the right cancel each other, and both directions are characterized by the same transitions probabilities. The existence of the second minimum breaks this symmetry and makes transition probabilities direction dependent. The memory of the initial state makes the walk turn back. During this process, the walker exerts forces on the environment. The more localized the initial distribution at a specific site the greater the memory effects that a walker has. If instead of a prepared state localized at the first minimum we had a uniform distribution along the pathway of the machine, a second average with respect to all the positions would be necessary in order to calculate the probability distribution, and the resulting exerted force would be smaller than for the perfectly localized initial state.

The exerted force in time has a maximum that depends on the temperature of the system. At 298 K, and for $\Delta x = 6 \text{ \AA}$, the exerted force is similar to that of biological molecular motors [48]. In Table 3, the maximum value of exerted forces for different space steps, stride of the walker, and for different temperatures is listed.

Table 3. Maximum value of exerted force for different strides of the walker and for various temperatures.

$\Delta x \text{ (\AA)}$	T=298°K	T=310°K	T=320°K
	$F_{\max} \text{ (pN)}$	$F_{\max} \text{ (pN)}$	$F_{\max} \text{ (pN)}$
1	0.354	0.129	0.062
2	1.654	0.599	0.290

3	3.24	1.191	0.579
6	6.24	2.355	1.149

To obtain a larger force the stride of the walker must be as large as possible. As pointed out before [44], the space step can have a physical meaning and must not be confused with the length of the pathway walked by the system. As the temperature goes up, the maximum exerted force decreases in agreement with the picture outlined in the discussion of figure 2a where at higher temperatures, backscattering from the deeper minimum has a higher chance to occur.

An important issue is the work produced in the process and the efficiency of the system. For $\Delta x = 6 \text{ \AA}$, at 298/310/320K the work is 0.264/0.0364/0.0084 kcal mol⁻¹. This is a fraction of the available free energy of 4 kcal mol⁻¹, and gives an efficiency of 6.6/0.91/0.21% for the three different temperatures. If the maximum exerted force was constant during the time needed for the initial population to pass from the first to the second minimum, as it is usually done in the frequently used phenomenological models, then the amount of energy needed for this would be equal to 0.5388/0.2028/0.0992 kcal mol⁻¹, which would give a yield of 13.47/5.07/2.48 % at 298/310/320 K. Notice that all the work produced by the walker would here be dissipated as viscous heat and cannot be used for any task unless there is coupling to an external load/system.

In figure 2(c), the work efficiency is shown, for three different temperatures. The efficiency is calculated with respect to the maximum work available of 4 kcal mol⁻¹ and for stride $\Delta x = 6 \text{ \AA}$ has a maximum value of 6.6 % at 298 K. It becomes 7.2/30.6 times smaller as the temperature is increased by 12/22 K. For space steps of $\Delta x = 1, 2$ and 3 \AA the efficiency at 298K is 0.0055, 0.110 and 0.582 % and becomes 6.8/28, 7.3/31.4 and 7.4/32.3 times smaller as the temperature is increased by 12/22 K. The rather low efficiency of the present system deserves a closer scrutiny, which can be done by considering the production of entropy.

Figure 2(d) shows the entropy production as a function of time. Initially, the entropy increases and the larger the temperature the greater and faster the entropy production. Entropy production is connected to the possibility that the walker visits the available space and to larger temperatures. Eventually, the entropy production decreases and entropy reaches a constant value. At a lower temperature, the final value of the entropy is smaller. As temperature goes down, the time derivative of the entropy in time, figure not showed, is faster

(and goes to zero when equilibrium is reached). The low efficiency and the low yield of work produced by the walker is due to high entropic losses. To understand it, let us consider in more detail the case of $T=298$ K. The walker reaches for the first time the second minimum after 0.2 ns. However, full localization on it -or equilibrium- is achieved only after 100 nsec. The several visits in and out of the second well imply the transformation of large amount of energy into heat.

Table 4 summarizes the results for three different systems where the walker is initially located at a well of different energy and the final well has a deeper depth of -14 kcal mol⁻¹. The maximum force is a function only of the depth of the final well. This trend agrees with the intuitive notion that the force is exerted mainly when the particle glides down the potential energy curve. Analogously, the useful work is also only a function of the minimum reached at equilibrium, while the efficiency increases as the energy differences of the two minima decreases.

Table 4. Maximum exerted force, F_{\max} (pN), efficiency, f (%), useful work, W (kcal mol⁻¹), for a stride or space step $\Delta x=6$ Å. The three different systems are labeled in terms of their energy minima, 7-14 kcal mol⁻¹, 10-14 kcal mol⁻¹, and 12-14 kcal mol⁻¹.

T (K)	7-14 kcal mol ⁻¹		
	F_{\max}	f (%)	W
298	6.242	3.775	0.26425
310	2.353	0.521	0.03647
320	1.149	0.12	0.0084
	10-14 kcal mol ⁻¹		
	F_{\max}	f (%)	W
298	6.24	6.607	0.26428
310	2.35	0.911	0.03644
320	1.1486	0.211	0.00844
	12-14 kcal mol ⁻¹		
	F_{\max}	f (%)	W
298	6.2417	13.26	0.2652
310	2.3534	1.824	0.03648
320	1.1486	0.422	0.00844

In a separate series of calculations, we determined the maximum exerted force as a function of the pathway length between the two minima. The longer the pathway length the smaller the maximum exerted force and the efficiency of the system. For example, in the 10-14 kcal mol⁻¹ system, the maximum force is 6.24 pN for a pathway length of 6 Å and 1.65 pN for a pathway length of 18 Å (the stride in both cases was $\Delta x = 6$ Å). The corresponding efficiency of the system drops from 6.6 % to 0.99 %. These variations are of entropic origin and set the limits under which Brownian motion can be converted into a directional one through the exploitation of spatio-temporal asymmetric, off equilibrium systems. In practice, a molecular machine works better if the distance between the two operating wells is as short as possible, otherwise entropy “washes out” its functioning.

5. Simple rules for design of elementary machines and conclusion

Important models have been proposed and discussed with the intent of calculating dynamical quantities of individual molecular machines [49-51]. The discrete stochastic Markovian model used here describes the dynamics of some of them. The time dependent probability distribution is determined and properties of the system are extracted. At room temperature and for a large stride of the walker, the maximum force that a walker exerts for a 10-14 kcal mol⁻¹ system (see text) is of order of several pN, while the efficiency of the process is of several percentage points. These values differ markedly from what could be estimated when the force is calculated as the ratio of the free energy gained by the motion (4 kcal mol⁻¹) divided the pathway length between the two minima. The difference becomes greater as the temperature increases and is mainly due to the Brownian motion that the system attempts to and does rectify. In practice, before reaching equilibrium, the walker visits the final well several times. In turn, the erratic motion of the particle generates entropy, which effectively depletes the maximum force deliverable by the machine.

A few simple rules to maximize the output in terms of force or efficiency emerge from this work and are applicable to the design of new molecular motors:

- (0) The available free energy divided by the length of the pathway offers only a rough upper value of the force that the machine exerts when it rectifies the Brownian motion: entropic effects strongly decrease the maximum possible force and they are mainly due to backscattering from the final equilibrium configuration,

- (1) A deeper well towards which the strider walks generates a larger force, also because it minimizes the probability of backscattering,
- (2) Entropy losses are crucial to undermine the efficiency of the system: they are minimal when the initial and final wells have the same energy,
- (3) The stride of the machine/walker should be as long as possible because it minimizes the number of accessible states and therefore the entropy. Such stride, Δx , is not the total length of the pathway, which actually must be as short as possible, but is the minimum step that the walker must overcome in its motion towards equilibrium. For instance, this step could be a base pair in DNA polymerases, or a phenyl group or a methylene group in some artificial molecular machines.

References

- [1] M. V. Smoluchowski, Experimentell nachweisbare, der üblichen Thermodynamik widersprechende Molekularphänomene, *Physik. Z.* **13** (1912) 1069–1080.
- [2] R. P. Feynman, R. B. Leighton, M. Sands, *The Feynman Lectures on Physics*, Addison-Wesley, Reading, 1966.
- [3] R. D. Astumian, P. B. Chock, T. Y. Tsong, Y. D. Chen, H. V. Westerhoff, Can free energy be transduced from electric noise? *Proc. Natl. Acad. Sci. U.S.A.* **84** (1987) 434–438.
- [4] M. Magnasco, Forced thermal ratchets, *Phys. Rev. Lett.* **71** (1993) 1477–1481.
- [5] J. Prost, J. Chauwin, L. Peliti, A. Ajdari, Asymmetric pumping of particles, *Phys. Rev. Lett.* **72** (1994) 2652–2655.
- [6] H. X. Zhou, Y. D. Chen, Chemically driven motility of Brownian particles, *Phys. Rev. Lett.* **77** (1996) 194–197.
- [7] R. D. Astumian, Thermodynamics and kinetics of a Brownian motor, *Science* **276** (1997) 917–922.
- [8] M. Kosmas, E. Bakalis, Diffusive motion in the presence of an array of interacting centers, *Phys. Lett. A* **358** (2006) 354–357.
- [9] J. F. Stoddart, Molecular machines, *Acc. Chem. Res.* **34** (2001) 410–411.
- [10] C. A. Schalley, K. Beizai, F. Vogtle, On the way to rotaxane-based molecular motors: Studies in molecular mobility and topological chirality, *Acc. Chem. Res.* **34** (2001) 465–476.
- [11] E. R. Kay, D. A. Leigh, F. Zerbetto, Synthetic molecular motors and mechanical machines, *Angew. Chem. Int. Ed.* **46** (2007) 72–191.
- [12] E. M. Perez, D. T. F. Dryden, D. A. Leigh, G. Teobaldi, F. Zerbetto, A generic basis for some simple light-operated mechanical molecular machines, *J. Am. Chem. Soc.* **126** (2004) 12210.
- [13] J. D. Badjic, V. Balzani, A. Credi, S. Silvi, J. F. Stoddart, A molecular elevator, *Science* **303** (2004) 1845.

- [14] M. E. Fisher, A. B. Kolomeisky, The force exerted by a molecular motor, *Proc. Nat. Acad. Sci. USA* **96** (1999) 6597–6602.
- [15] A. Stolow, D. M. Jonas, Multidimensional snapshots of chemical dynamics, *Science* **305** (2004) 1575–1577.
- [16] M. R. Panman, P. Bodis, D. J. Shaw, B. H. Bakker, A. C. Newton, E. R. Kay, A. M. Brouwer, W. Jan Buma, D. A. Leigh, S. Woutersen, Operation mechanism of a molecular machine revealed using time-resolved vibrational spectroscopy, *Science* **328** (2010) 1255.
- [17] N. Koumura, R.W.J. Zijlstra, R. A. van Delden, N. Harada, B. L. Feringa, Light-driven monodirectional molecular rotor, *Nature* **401** (1999) 152–155.
- [18] W. Feller, *Introduction to Probability Theory and Its Applications*, Wiley, New York, 1971.
- [19] E. Bakalis, C. Vlahos, M. Kosmas, Diffusion in the presence of a pole: From the continuous Gaussian to a discrete lattice model, *Physica A* **360** (2006) 1–16.
- [20] R. Feynman, A. Hibbs, *Quantum Mechanics and Path Integrals*, McGraw-Hill, New York, 1965.
- [21] K. F. Freed, *Renormalization Group Theory of Macromolecules*, Wiley, New York, 1987.
- [22] M. Chaichian, A. Demichev, *Path Integrals in Physics, Vol.1: Stochastic Processes and Quantum Mechanics*, Institute of Physics Publishing, Bristol and Philadelphia, 2001.
- [23] H. D. Ursell, The evaluation of Gibb’s phase-integral for imperfect gases, *Proc Cambridge Phil. Soc.* **23** (1927) 685–697.
- [24] J. E. Mayer, The statistical mechanics of condensing systems I, *J. Chem. Phys.* **5** (1937) 67–73.
- [25] M. Fixman, Excluded volume in polymer chains, *J. Chem. Phys.* **23** (1955) 1656–1659.
- [26] M. Fixman, Erratum: Excluded volume in polymer chains, *J. Chem. Phys.* **24** (1956) 174–174.
- [27] P. Erdős, R. C. Herndon, Theories of electrons in one-dimensional disordered systems, *Adv. Phys.* **31** (1982) 65–163.
- [28] D. A. Leigh, J. K. Y. Wong, F. Dehez, F. Zerbetto, Unidirectional rotation in a mechanically interlocked molecular rotor, *Nature* **424** (2003) 174–179.
- [29] F. G. Gatti, S. Leon, J. K. Y. Wong, G. Bottari, A. Altieri, M. A. Morales Farran, S. J. Teat, C. Frochot, D. A. Leigh, A. M. Brouwer, F. Zerbetto, Photoisomerization of a rotaxane hydrogen bonding template: Light-induced acceleration of a large amplitude rotational motion, *Proc. Natl. Acad. Sci. USA* **100** (2003) 10–14.
- [30] D. A. Leigh, A. Troisi, F. Zerbetto, Reducing molecular shuttling to a single dimension, *Angew. Chem. Int. Ed.* **39** (2000) 350–353.
- [31] O. Bilek, L. Skala, Exact propagator for coherent motion of excitons in a linear chain with one impurity, *Phys. Lett. A* **119** (1986) 300–303.
- [32] V. I. Kovanis, V. M. Kenkre, Exact self-propagators for quasiparticle motion on a chain with alternating site energies or intersite interactions, *Phys. Lett. A* **130** (1988) 147–150.
- [33] X. G. Zhao, Total propagator probability for an exciton moving on a linear chain with one impurity, *Phys. Lett. A* **165** (1992) 257–259.

- [34] S. M. Blinder, Green's function and propagator for the one-dimensional δ -function potential, *Phys. Rev. A* **37** (1988) 973–976.
- [35] A. Szabo, G. Lamm, G. H. Weiss, Localized partial traps in diffusion processes and random walks, *J. Stat. Phys.* **34** (1984) 225–238.
- [36] P. K. Datta, A. M. Jayannavar, Statistical properties of the nearest-neighbour distance at a single imperfect trap, *Phys. A* **184** (1992) 135–142.
- [37] H. Taitelbaum, One-dimensional δ -function potential and the radiation boundary condition, *Phys. A* **190** (1992) 295–302.
- [38] M. A. Rodriguez, G. Abramson, H. S. Wio, A. Bru, Diffusion-controlled bimolecular reactions: Long-and intermediate- time regimes with imperfect trapping within a Galanin approach, *Phys. Rev. E* **48** (1993) 829–836.
- [39] T. J. Newman, W. Triampo, Binary data corruption due to a Brownian agent, *Phys. Rev. E* **59** (1999) 5172–5186.
- [40] B. Derrida, Velocity and diffusion constant of a periodic one-dimensional hopping model, *J. Stat. Phys.* **31** (1983) 433–450.
- [41] E. Bakalis, Designing nanomachines: A theoretical and computational approach, *J. Comput. Theor. Nanosci.* **7** (2010) 1783–1799.
- [42] U. Seifert, Entropy production along stochastic trajectory and an integral fluctuation theorem, *Phys. Rev. Lett.* **95** (2005) 040602-4.
- [43] I. Derenyi, M. Bier, R. D Astumian, Generalized efficiency and its application to microscopic engines, *Phys. Rev. Lett.* **83** (1999) 903–906.
- [44] Y. R. Chemla, J. R. Moffitt, C. Bustamante, Exact solutions for kinetic models of macromolecular dynamics, *J. Phys. Chem. B* **112** (2008) 6025–6044.
- [45] U. K. Demirok, R. Laocharoensuk, K. M. Manesh, J. Wang, Ultrafast catalytic alloy nanomotors, *Angew. Chem. Int. Ed.* **47** (2008) 9349–9351.
- [46] M. Schulz, S. Stepanow, Random walks in glasslike environments, *Phys. Rev. B* **59** (1998) 13528–13530.
- [47] G. M. Schutz, S. Trimper, Elephants can always remember: Exact long-range memory effects in a non-Markovian random walk, *Phys. Rev. E* **70** (2004) 045101(R)-4.
- [48] J. T. Finer, R. M. Simmons, J. A. Spudich, Single myosin molecule mechanics: piconewton forces and nanometre steps, *Nature* **368** (1994) 113–119.
- [49] R. D. Astumian, Adiabatic operation of a molecular machine, *Proc. Natl. Acad. Sci. USA* **104** (2007) 19715–19718.
- [50] R. D. Astumian, Design principles for Brownian molecular machines: how to swim in molasses and walk in hurricane, *Phys. Chem. Chem. Phys.* **9** (2007) 5067–5083.
- [51] R. Eelkema, M. M. Pollard, J. Vicario, N. Katsonis, B. Serrano Ramon, C. W. M. Bastiaansen, D. J. Broer, B. L. Feringa, Nanomotor rotates microscale objects, *Nature* **440** (2006) 163.

Supporting Information

Section A

It is worth providing an example of the application of equation (2). The walker starts from site $x=0$ on a $1\overline{D}$ path characterized by two potential wells located at $x=2$ and $x=4$ which have temperature-weighted energies $u_{1,d}=-0.1$ and $u_{2,d}=-0.2$. After the first time-step, the walker can be at $x=-1$ or $x=1$ with equal probability $1/2$. Since neither site is home of a potential well, the total probability remains normalized. At the second step, the walker can be at positions $x=-2,0,2$. The sum of the probabilities after this step exceeds unity and must be re-normalized. Table A.1 provides an explicit description of the first four steps.

Table A.1. Probabilities and, in brackets, normalised probabilities at each site. They are obtained from the transition probabilities described in the “picture” section and given under each site in brackets.

Site	-4	-3	-2	-1	0	1	2	3	4	Normalization factor
Time step	$u=0$	$u=0$	$u=0$	$u=0$	$u=0$	$u=0$	$u=u_{1,d}$	$u=0$	$u=u_{2,d}$	
0	0	0	0	0	1	0	0	0	0	1
1	0	0	0	1/2 (1/2)	0	1/2 (1/2)	0	0	0	1
2	0	0	0.25 (0.2436)	0	0.5 (0.487)	0	0.2763 (0.2692)	0	0	1.0263
3	0	0.1218 (0.1218)	0	0.3652 (0.3652)	0	0.3781 (0.3781)	0	0.1346 (0.1346)	0	1
4	0.0609 (0.0585)	0	0.24355 (0.23381)	0	0.3717 (0.35683)	0	0.283311 (0.27198)	0	0.0822 (0.07891)	1.04166

Section B

In the path integral representation, the probability density distribution function, $P(x_B, t; x_A, 0)$, to find a diffusing particle, which performs random motion, in a site B at time t given its initial position, a site A , for $t=0$ is written

$$\begin{aligned}
 P(x_B, t; x_A, 0) = & \int_{-\infty}^{\infty} dx_1(t) \frac{\text{Exp}(-(x_1 - x_A)^2 / 4Dt_1)}{\sqrt{4\pi Dt_1}} \int_{-\infty}^{\infty} dx_2(t) \frac{\text{Exp}(-(x_2 - x_1)^2 / 4D(t_2 - t_1))}{\sqrt{4\pi D(t_2 - t_1)}} \dots \\
 & \dots \int_{-\infty}^{\infty} dx_n(t) \frac{\text{Exp}(-(x_n - x_{n-1})^2 / 4D(t_n - t_{n-1}))}{\sqrt{4\pi D(t_n - t_{n-1})}} \delta(x_n(t) - x_B)
 \end{aligned}
 \tag{B.1}$$

where, the delta function on the integral ensures that the diffusing particle will be in site B at time t . This function is called pure Wiener measure and is written as

$$P(x_B, t; x_A, 0) = \int D[x(\tau)] \text{Exp} \left[-\frac{1}{4D} \int_0^t d\tau (dx(\tau)/dt)^2 \right] \quad (\text{B.2})$$

where, $D[x(\tau)]$ is the measure of the differential of the path integral, while the integrand in the exponential term is corresponded to kinetic term.

The term $\left(1/\sqrt{4\pi D(t_i - t_{i-1})}\right) \text{Exp} \left[-(x_i - x_{i-1})^2 / (4D(t_i - t_{i-1})) \right]$ of equation (B.1) is called transition probability density, and is integrated over the whole space at each possible step. If extra interactions, potential sites, are present in the area in which a random motion occurs then the transition probability is modified to include these terms, and reads

$$P(x_i, t_i; x_{i-1}, t_{i-1}) = \left(\frac{1}{\sqrt{4\pi D(t_i - t_{i-1})}} \right) \text{Exp} \left[-\frac{(x_i - x_{i-1})^2}{4D(t_i - t_{i-1})} - \frac{V(x_i(t) - x_s)}{k_B T} \right] \quad (\text{B.3})$$

Extra interactions are activated by the term $V(x_i(t) - x_s)$ where, x_s are the positions of the potential sites, and $x_i(t)$ is the time dependent trajectory of the diffusing particle. $V(x_i(t) - x_s)$ is a function of the relative distance between the position of the particle and the position of the site. A simplification could be made in order to replace the true potential with a mean field potential. A first approximation to any kind of central potential is this of delta function. As it has been shown a real potential, $V(x_i(t) - x_s)$, can be replaced by $u_c \delta(x_i(t) - x_s)$ where

$$u_c = \int_0^\infty dx \left(1 - \text{Exp}[-V(x)/k_B T] \right) \quad (\text{B.4})$$

and x is the relative distance between diffusing particle and potential site, while the subscript c stands for continuum space. For example, a single potential well of width Δx and depth $-\varepsilon$ can be described by $u_c = \Delta x \text{Exp}(\varepsilon/k_B T)$, where u_c bears units of volume in general or length for the one-dimensional case.

Inserting delta function potential into equation (B.3), we write

$$P(x_i, t_i; x_{i-1}, t_{i-1}) = \left(\frac{1}{\sqrt{4\pi D(t_i - t_{i-1})}} \right) \text{Exp} \left[-\frac{(x_i - x_{i-1})^2}{4D(t_i - t_{i-1})} - u_c \delta(x_i(t) - x_s) \right] \quad (\text{B.5})$$

Expanding (B.5) regarding to interaction potential, we write

$$P(x_i, t_i; x_{i-1}, t_{i-1}) = \left(\frac{1}{\sqrt{4\pi D(t_i - t_{i-1})}} \right) \text{Exp} \left[-\frac{(x_i - x_{i-1})^2}{4D(t_i - t_{i-1})} \right] \sum_{n=0}^{\infty} \frac{(-u_c)^n}{n!} (\delta(x_i(t) - x_s))^n \quad (\text{B.6})$$

The factor n in the above expansion shows the number of visits of diffusing particle in the potential site. For $n=0$, there is no contact between particle and potential site and the transition probability density for the free case is returned. For $n=1$, the trajectory traced by the diffusing particle between two points in space has one common point with the potential site, two for $n=2$, and so on for bigger values of n . The probability density function of a diffusing particle to be found on a site B given its starting position, site A , in the presence of a potential site, reads

$$P(x_B, t; x_A, 0) = \int D[x(\tau)] \text{Exp} \left[-\frac{1}{4D} \int_0^t d\tau (dx(\tau)/d\tau)^2 - \int_0^t \bar{u}_c \delta(x(\tau) - x_s) d\tau \right] \quad (\text{B.7})$$

Under the time integral, the interaction potential, u_c , has been converted to a frequency factor, \bar{u}_c , which bears units of length per time. Let assume a time dependent trajectory traced by a diffusing particle between two points in space, A and B , at time t , which has only one common point with the potential site. By the classical definition, the probability to find a diffusing particle at point B at time t given its initial position, point A at time 0, is equal to all trajectories connect these two sites, A and B at time t , divided by all possible trajectories traced by the particle since started from point A . Trajectories that connect A and B at time t can be divided in two categories. Trajectories that do not have common point with the potential site, S , and are equal weighted giving the classical Gaussian distribution,

$$P_1(x_B, t; x_A, 0) = u_c \frac{\text{Exp}[-(x_B - x_A)^2 / (4Dt)]}{\sqrt{4\pi Dt}} \quad (\text{B.8})$$

and trajectories with one common point with the potential site. We split the time trajectory in N -segments of time τ , such that $N\tau=t$, and we write

$$0 < t_1 < t_2 < t_3 < \dots < t_{n-1} < t_n \text{ with } t_i - t_{i-1} = \tau, \quad i = 1, 2, 3, \dots, n \quad (\text{B.9})$$

The contact between diffusing particle and potential site can be done any time moment that belongs to the range $[0, t]$. The contact can be done during the first step, t_1 , or during the second step, t_2 , or during the third step and so on. Thus, we have n possible contacts, which are done during different time steps. If during time step t_i the contact between diffusing

particle and potential site is true then the probability density distribution function is written as, where $n-1$ integrals have been carried out,

$$P_2(x_B, t; x_A, 0) = u_c \frac{\text{Exp}[-(x_S - x_A)^2 / (4Dt_i)]}{\sqrt{4\pi Dt_i}} \frac{\text{Exp}[-(x_B - x_S)^2 / (4D(t - t_i))]}{\sqrt{4\pi D(t - t_i)}} \quad (\text{B.10})$$

All the different time moments in which there is contact must be taken into account, thus the probability density is a time average all over the different time moments divided by the number of different ways, and it reads

$$P_2(x_B, t; x_A, 0) = u_c \frac{1}{N\tau} \sum_{i=1}^N \frac{\text{Exp}[-(x_S - x_A)^2 / (4Dt_i)]}{\sqrt{4\pi Dt_i}} \frac{\text{Exp}[-(x_B - x_S)^2 / (4D(t - t_i))]}{\sqrt{4\pi D(t - t_i)}} \quad (\text{B.11})$$

As the time step is infinitesimal small, tends to zero, the sum is converted to integral

$$P_2(x_B, t; x_A, 0) = \bar{u}_c \int_0^t dt_i \frac{\text{Exp}[-(x_S - x_A)^2 / (4Dt_i)]}{\sqrt{4\pi Dt_i}} \frac{\text{Exp}[-(x_B - x_S)^2 / (4D(t - t_i))]}{\sqrt{4\pi D(t - t_i)}} \quad (\text{B.12})$$

The total probability density function to find a particle, which performs random motion, in site B knowing that started from site A is written as $P(x_B, t; x_A, 0) = P_1(x_B, t; x_A, 0) + P_2(x_B, t; x_A, 0)$, and it is not normalized to unity anymore. The normalized probability is taken from the division of the un-normalized probability distribution with the factor $C(t) = \int P(x, t; x_A, 0) dx$, which includes the contributions from all possible trajectories traced by the particle at the same time. In equation (B.12), the term $\bar{u}_c = u_c / t_{eq}$ has been defined, where t_{eq} is a time needed for the diffusing particle to be already in equilibrium state. A choice of $t_{eq} = 1 \text{ sec}$ is reasonable, in practice; nanomachines reach equilibrium much faster than 1 sec. Of course, any other choice of t_{eq} is accepted since the final description of the process is not affected, as the presence of potential makes the probability distribution non-normalized, and the normalized probability includes both in numerator and denominator the factor \bar{u}_c .